

POSITION DEPENDENCY OF SURFACE ROUGHNESS IN PARTS FROM LASER BEAM MELTING SYSTEMS

S. Kleszczynski¹, A. Ladewig², K. Friedberger², J. zur Jacobsmühlen³, D. Merhof³, G. Witt¹

¹ Chair of Manufacturing Technology, Institute for Product Engineering, University of Duisburg-Essen, Germany

² MTU Aero Engines AG, Germany

³ Institute of Imaging and Computer Vision, RWTH Aachen University, Germany

REVIEWED

Abstract

Laser Beam Melting is a promising Additive Manufacturing technology for the production of complex metal components. During batch production of multiple identical parts in a single build job, we observed parts with deviating surface roughness in certain areas, which all faced away from the laser. This suggests a dependency of surface roughness on the part position in the build chamber. In this work we systematically reproduce and analyze this effect. We place hollow pyramids with twelve faces and two different overhanging angles at nine positions on the substrate plate and build this setup twice, using an imaging setup for process documentation. Surface roughness is measured by contact profilometry on three lines for each pyramid face. Our experiments reproduce the effect. Based on these findings we present a hypothesis for the cause and show metallographic images to support our theory. As a consequence, the position relative to the laser should be considered in the design phase for parts with high surface quality requirements.

1. Introduction

Nowadays, Additive Manufacturing (AM) is on its way to become an established manufacturing technology. The main characteristic of AM technologies is the layer by layer production of three dimensional components based on CAD data. It is widely accepted, that AM technologies are able to produce high complexity parts in shorter production times compared to conventional manufacturing processes [1]. Beside applications in the area of prototyping during product development or the production of tooling devices, AM processes offer huge potential for small batch production of industrial high performance components [2]. Laser Beam Melting (LBM), which is often designated as Selective Laser Melting (SLM), Direct Metal Laser Sintering (DMLS) or Direct Metal Printing (DMP), is a powder bed based AM technology. In a first step of the LBM process a thin layer of metal powder is applied onto a build platform. Next the powder is selectively melted by a laser beam, which scans the powder bed according to the current cross section of one or more three dimensional CAD models. After that, the build platform is lowered and the first two process stages are repeated iteratively until the build process is finished and all components are produced. Due to the focused energy input into a small volume, the powder fully melts and solidifies into approximately 100 % dense bulk material [1], [3], [4]. It has been reported, that the mechanical properties of LBM components are widely comparable to conventionally processed materials [5]. To exploit the technological progress and economic potential of novel innovative LBM applications, industrial and academic research efforts focus on the implementation of LBM technologies into industrial applications. Due to high safety requirements in promising fields of application, the development of suitable quality management and process monitoring systems is a crucial issue for further establishment of the LBM technology.

Due to potential reductions of production costs and especially the economic benefit of innovative lightweight designs, LBM is of great interest for aerospace and aero engine industry. MTU Aero Engines AG established a first LBM production line for the batch production of a boroscope boss, which is an auxiliary part on the outside of the case of a low pressure turbine [6]. Considering the crucial need of expedient quality assurance, different approaches are used, which cover the whole process chain and provide destructive and non-destructive testing of materials, qualification of process parameters and online process monitoring [7]. During process parameter studies a significant divergence of surface roughness was observed. Further investigations

indicated that the severity level of surface roughness fluctuations depends on the specimen position and orientation within the process chamber. Furthermore it was observed that surface roughness increases for 45° overhanging surfaces which face away from the center of the process chamber, respectively the laser window. It is known that, due to adhesion of powder particles and other effects, surface roughness of LBM components still requires improvement of process parameters or post processing steps for some applications. Nevertheless, industrial implementation of LBM requires reliable and reproducible mechanical properties. In order to examine the observed fluctuations a hypothesis was formulated which implied, that there might exist an interdependency between the part position in the process chamber, the overhanging angle, the orientation of the surface and the resulting surface roughness. This is remarkable as most commercial LBM systems are equipped with f-theta lenses, which should ensure a uniform beam diameter and scanning speed at every position of the process chamber [8]. The aim of this paper is to provide a systematical analysis of the observed effect and to propose a hypothesis for the cause.

2. State of the Art

Compared to conventional manufacturing processes LBM components have relatively poor surface qualities. The surface roughness is in the order of 10 µm to 100 µm – depending on the surface overhanging angle - in the as-built condition [1]. This is in a way unavoidable, due to the powder bed based principle of LBM. There is no sharp boundary between the melting region and the adjacent powder particles. Instead there is a transition zone in which the intensity of the beam source decreases. Most commercial LBM systems use a Gauss profile laser beam source. Newer LBM systems use a top hat beam profile, in order to improve the volume build rate and to reduce process costs [9].

The main factors influencing surface quality in LBM processes are adhesions of powder particles, melt extensions during consolidation, stair step effects, balling formation, weld sputtering, elevated part regions and the impact of the interface region of support structures [3]. Especially overhanging structures are frequently affected by inferior surface quality. Due to the about three orders of magnitude lower thermal conductivity of metallic powder compared to metallic bulk material [4], heat accumulation could induce balling extensions of melt traces and adhesion of powder particles at such overhanging structures [10], [11]. Depending on the overhanging angle and the powder thickness, stair step effects have also to be taken into consideration [12].

To analyze interdependencies related to the formation of surface roughness during LBM, the basic physical principles have to be discussed. Kruth et al. [13] stated that the main driving forces during consolidation are temperature effects, gravity and capillary forces. Depending on the process and material parameters, wetting of the solidified material can be insufficient leading to a lack of fusion, which finally induces increased porosity. Another known consolidation phenomenon is the earlier mentioned “balling” effect. When “balling” occurs the melt pool breaks up into spherical structures [13] which may also cause enhanced porosity, increased top/side surface roughness [12], [14] or elevated part regions [10].

In [15] the impact of the stochastic nature of powder particle distribution on surface quality and binding defects is presented. The authors propose a numerical simulation model, which allows estimating the impact of different process parameter configurations on the resulting shape deviations and binding defects for thin vertical walls. To take the random characteristic of particle distribution inside the powder bed into account the “rain model packing algorithm” was used for the simulation. The described experimental work was exemplarily carried out for the Electron Beam Melting (EBM) process, which differs from LBM in that an Electron Beam is used for melting. The simulation results and the experimental validation showed that especially the high surface tensions of the molten powder material in combination with wetting of stochastic, loosely packed powder particles are relevant for the cause of the high surface roughness. Furthermore, both the simulation and the experimental results, showed that surface roughness is always much higher than the mean powder particle diameter. This rules out a sole dependency between surface roughness and powder particle distribution and implies that melting, wetting and solidification effects could dominate the manifestation of surface roughness. Moreover the authors point out that position accuracy of the scanning system and the beam quality should also be taken into consideration, since these also affect the manifestation of thermal evolution. Additionally it is stated, that the improvement of the surface roughness is eventually limited by the stochastic nature of the powder bed.

Nevertheless several works have developed strategies for optimizing surface roughness. Mumtaz [14] investigates the influence of pulsed laser exposure on top and side surface roughness. The presented results showed that adapted process parameters can in principle reduce negative effects like balling or insufficient wetting. At the same time, however, the orientation of surfaces also seems to have a significant impact, since parameters that reduced side roughness increased top roughness. In [12] the effect of different sloping angles was examined for top surfaces. It is stated, that particle adhesion increases with increasing sloping angles due to larger number of stair steps. In consequence more powder particles are partially melted at the edges of stair steps, resulting in a rougher surface. Spierings et al. [2] reported that powder adhesion and the resulting surface roughness can be reduced when lower particle size distributions are used. Regarding the process parameters it was found, that scan velocities which produce good part densities tend to produce good surface qualities at the same time.

3. Experimental Setup

For experimental build processes we use an EOSINT M 270 LBM system by EOS GmbH. The powder material used was EOS NickelAlloy IN718, which is a nickel base alloy suitable for high temperature applications. The process parameters used were standard IN718 parameters as mentioned in [16]. Layer thickness was set at 20 μm . Surface roughness was measured using the profile method according to DIN EN ISO 4287 [17] and DIN EN ISO 4288 [18]. A Mitutoyo SJ-400 profilometer was used for surface roughness measurements. The average surface roughness, which is defined as:

$$R_z = \frac{1}{5} \sum_{i=1}^5 R_z(i)$$

was chosen for interpretation of measurements, due to its sensitivity to statistical outliers. All experimental build processes were documented using a high resolution imaging process documentation system as described in [10]. The acquired images were additionally analyzed to identify possible causes for the fluctuations of surface roughness.

Two different kinds of hollow pyramids geometries were selected as test specimen. The sides of the two specimens have an overhanging angle of 45° and 70° with respect to the horizontal substrate plate surface. Each hollow pyramid specimen features twelve surfaces at the inside and at the outside (see Figure 1a), which are rotated anti-clockwise in steps of 30°. The surface which faces the process chamber door is determined as 0° surface. In total this enables the measurement of 24 different orientated surfaces for each specimen. For statistical assurance each surface was measured three times. To examine the position dependency of surface roughness the substrate plate was separated in nine sections (see Figure 1b) and the different specimens were placed in the middle of these sections onto the substrate plate. To avoid disturbances of weld sputtering, powder coating and other possible effects during laser exposure every specimen was built in a separate build process. In order to exclude random process errors or effects at the specimens surface, the experimental setup was built twice, which means that 46 specimen were built and analyzed in total. To provide a clear assignment of specimen we chose to name the test specimen after their position in row and column. This means that specimens placed in the nearest row to the process chamber front door are labeled as “R1”, which means “row one”. Specimens which are positioned in the right column of the substrate plate are labeled as “CR”, which means “right column” (see Figure 1b). In order to provide a clear distinction of the different test series and overhanging angles of test specimen both labels were added in the specimen designation. A 45° overhanging specimen, which was built during test series 1 at the upper right corner of the substrate plate is distinguished as R3CR-45-1 (see Figure 1b).

For interpretation of measurement results the arithmetic mean of all three measurements per surface and the related standard deviation were determined (see Figure 2a). To provide a visual impression of the tendencies of surface roughness manifestations the measurement data was prepared in polar plots as exemplary shown in Figure 2b. In this figure profilometry results are prepared for specimen R3CR-45-1. Surface roughness values of the inner surfaces are depicted as blue markers, results of the outer surfaces are depicted as red markers. This makes it clear that the inner surface roughness shows some outliers, but stays in a constant range between 75 μm and 85 μm . The error bars indicate, that there were some outliers at the 60° and 240° surface. Whereas the results of the outer surface show a clear tendency of increased surface roughness, especially for the surface orientations

from 120° to 300°. Error bars indicate, that these tendency is not due to statistical outliers. As standard deviations were at the same level for all measurements, the polar plots were prepared without errors bars.

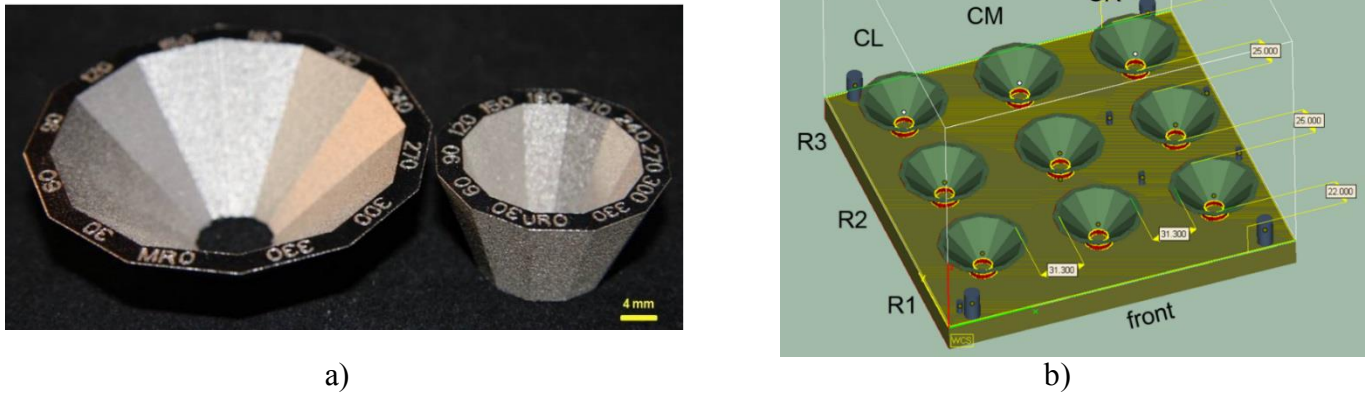


Figure 1: a) Selected specimen geometry: hollow twelve-sided frustum of a pyramid, which enables the measurement of surface roughness at the inner (upskin) and the outer (downskin) surface of the specimen. The test specimen on the left provides an overhanging angle of 45°. The specimen on the right provides 70°. For identification purpose the top surface was marked by the anti-clockwise degree of surface rotation in relation to the machine door. b) Specimen alignment at the substrate plate. Note that all specimen were built separately to avoid disturbing effects during exposure and powder coating.

In addition to the mentioned test series for each specimen the influence of post processing and thermal load on the deviations of surface roughness were meant to be examined too. Particle adhesion after melting of the contour regions is a known issue in LBM (see section 2). Blast cleaning provides an efficient post treatment of LBM components and is suitable for the removal of adherent powder particles. In order to examine the impact of powder particle adhesion on the observed fluctuation of surface roughness two selected 45° specimen which were positioned in the process chambers corners were blast cleaned and afterwards again analyzed by profilometry. Due to the physical principles of LBM it seems reasonable that the remaining fluctuations are caused by different thermal situations during the melting and consolidation process. In this context additional thin walled 45° specimen (0.5 mm wall thickness) were built in the corners of the process chamber to examine whether the geometrical characteristic of the parts cross section influences the heat conduction during solidification. Profilometry and data preparation for these additional specimen were carried out as mentioned above.

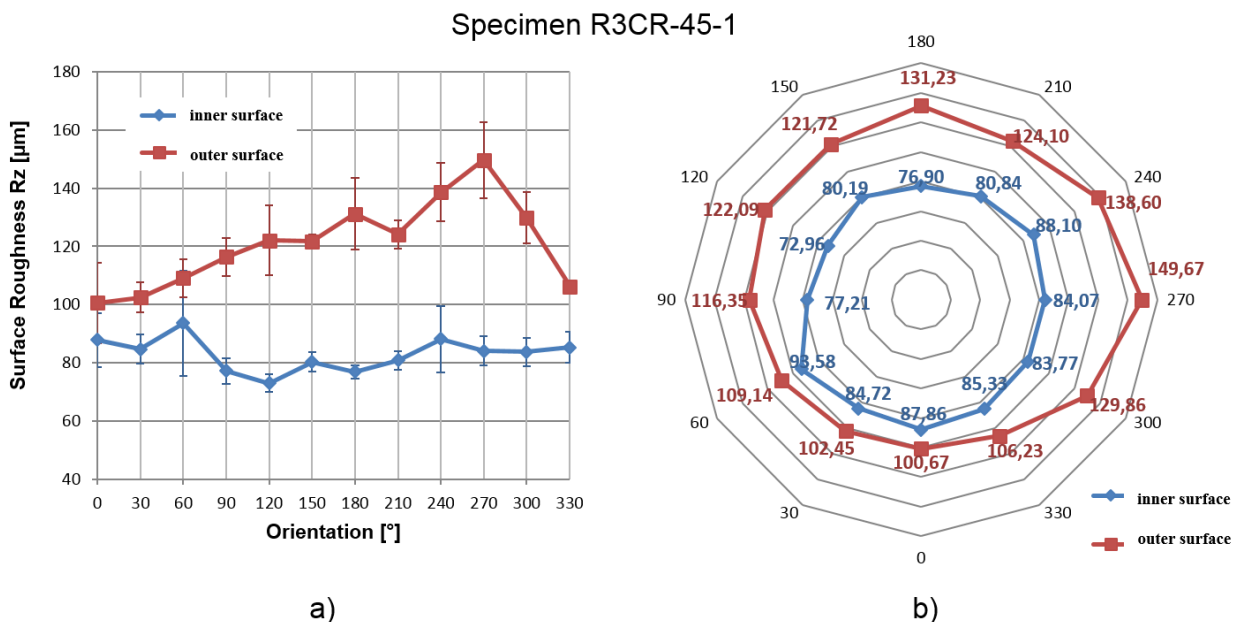


Figure 2: Graphical preparation of measurement data of test specimen R3CR 45-1. a) representation of measurement results as a function of surface orientation. Blue dots and lines represent the surface roughness value of the inner (upskin) specimen surfaces, respectively. Red dots and lines represent the measurement results of the outer (downskin) surfaces. Standard deviation markers were added to illustrate the statistical scattering of measurement data. b) Transformation of measurement data into a polar plot. Each surface orientation is represented by a single coordinate axis. Estimated values of surface roughness are plotted over the respective axis.

4. Results and Discussion

Interpretation of profilometry results

Figure 3 shows the summarized results of surface roughness measurements of test series 1 for the 45° specimen. The roughness of the outer surfaces is on an average higher than that of the inner surfaces, which is probably related to the increased formation of adhesion of powder particles and melt extensions at overhanging surfaces. Surfaces which are faced to the borders of the process chamber show increased roughness values compared to other orientations of the outer test surfaces. Surface roughness is enhanced in the order of 20 μm. In particular specimens R3CR-45-1, R2CR-45-1, R1CR-45-1 and R1CL-45-1 show strongly increased surface roughness values up to 53 μm.

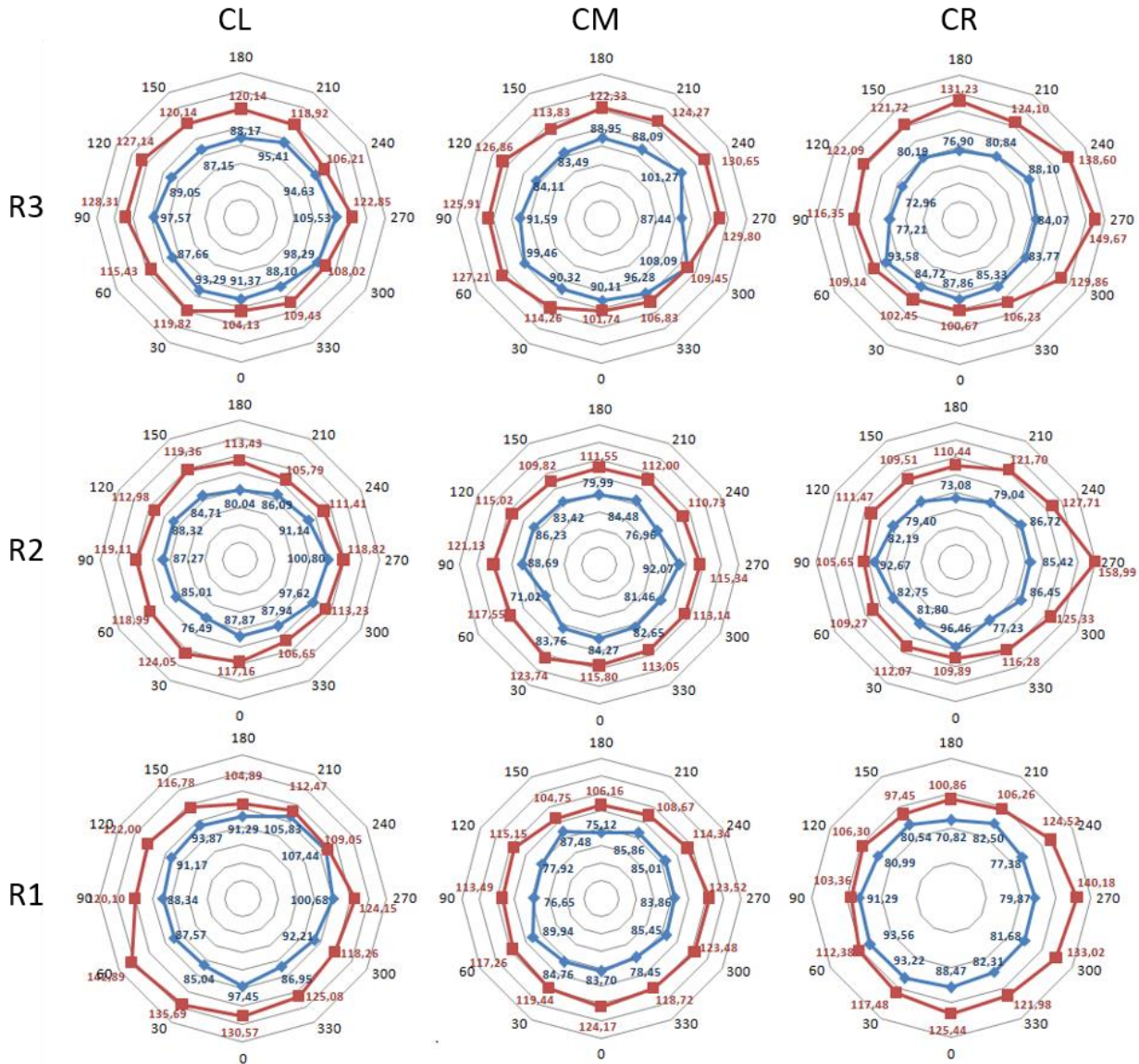


Figure 3: Summarized results of profilometry measurements of test series 1 for the 45° specimen. A clear tendency of increased surface roughness values at surfaces which are facing the walls of the process chamber can be observed.

Specimen R2CM-45-1 shows quite uniform roughness values at the outer surfaces. The maximum deviation of the outer surface roughness values at this specimen is 13,92 μm, which is in the range of standard deviation. The inner surface roughness for specimen R2CM-45-1 shows some deviations, which are not clearly associated to an obvious tendency and are thus probably related to the uncertainty of measurement. At the other specimens' inner surfaces an opposite tendency compared to the outer surfaces can be observed. Surface roughness of the inner surfaces is slightly increased for the surfaces facing the middle of the process chamber. In

contrast to the outer surfaces the increase of surface roughness is only in the order of 10 μm . Compared to standard deviations of the inner surfaces (see Figure 2a) this slight increase can be considered a proven tendency anyway.

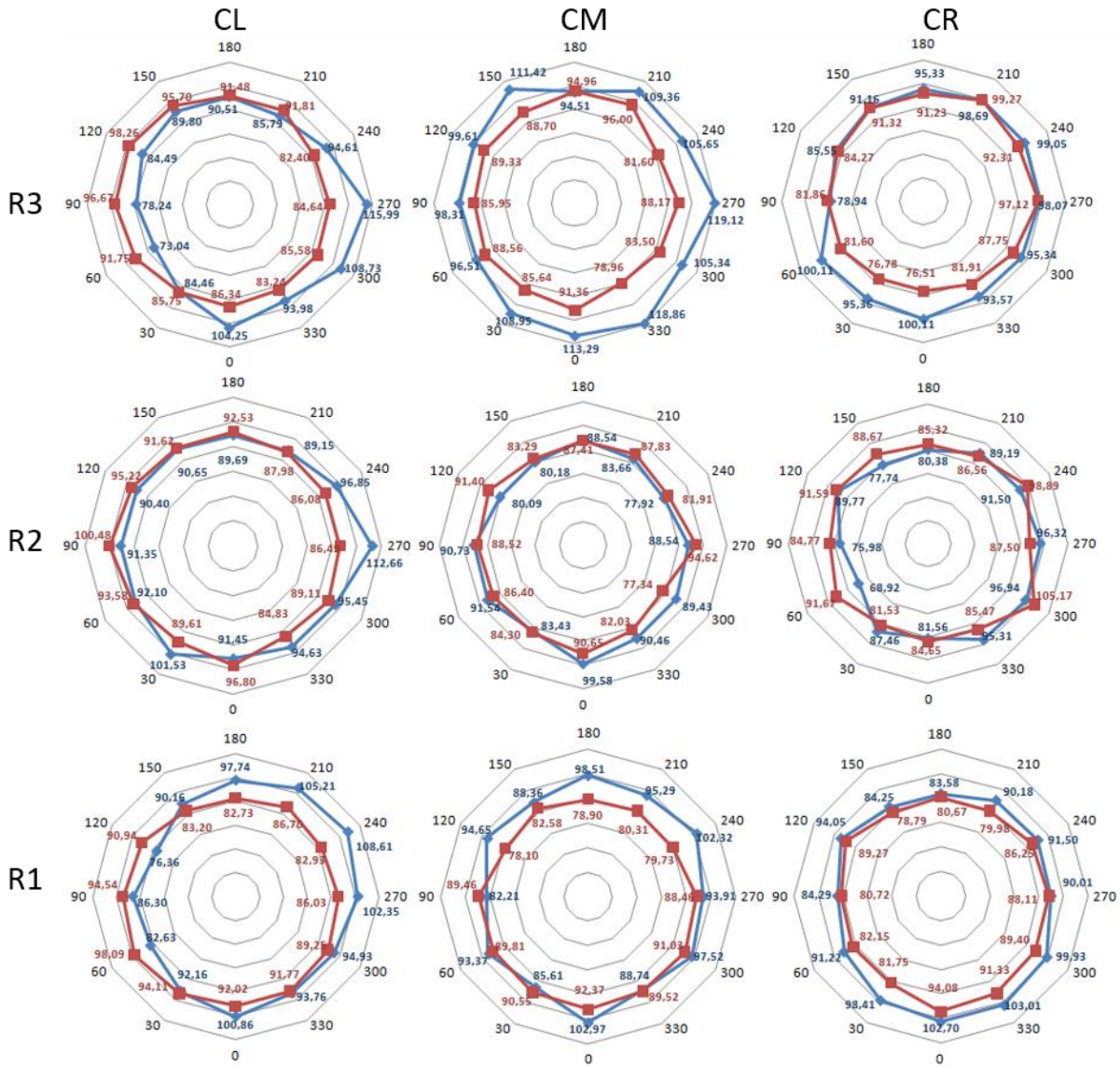


Figure 4: Summarized results of profilometry measurements of test series 2 for the 70° specimen. A slight tendency of increased surface roughness values at the inner surfaces oriented to the center of the process chamber is recognizable.

Figure 4 presents the summarized results of the 70° specimens of test series 2. As can be seen from the graphical preparation of measurement data the reduced overhanging angle seems to change the tendencies of surface roughness manifestation in a consistent manner. Most surfaces facing away from the center of the process chamber exhibit quite similar values. A slight increase of roughness can be observed at the inner surfaces which are orientated to the middle of the process chamber. The average increase is 10 μm , which is close to the standard deviations of the inner surface measurement results. This may explain why the suspected tendency does not occur for every specimen. Especially the results of specimens R1CR-70-1 and R2CR-70-1 do not show a clear manifestation of increased roughness values at the inner surfaces. The above presented results were selected exemplarily. The respective second test series of the two different types of specimen showed similar results, so that it can be stated that the observed tendencies are reproducible.

So far the conducted studies have shown an interdependency between surface orientation, part position and surface orientation for specimens with uniform wall thicknesses. Additionally it is pointed out, that all measurements refer to the as-built condition. In a next step additionally specimen were built and examined to illuminate further possible influencing factors of the observed effect.

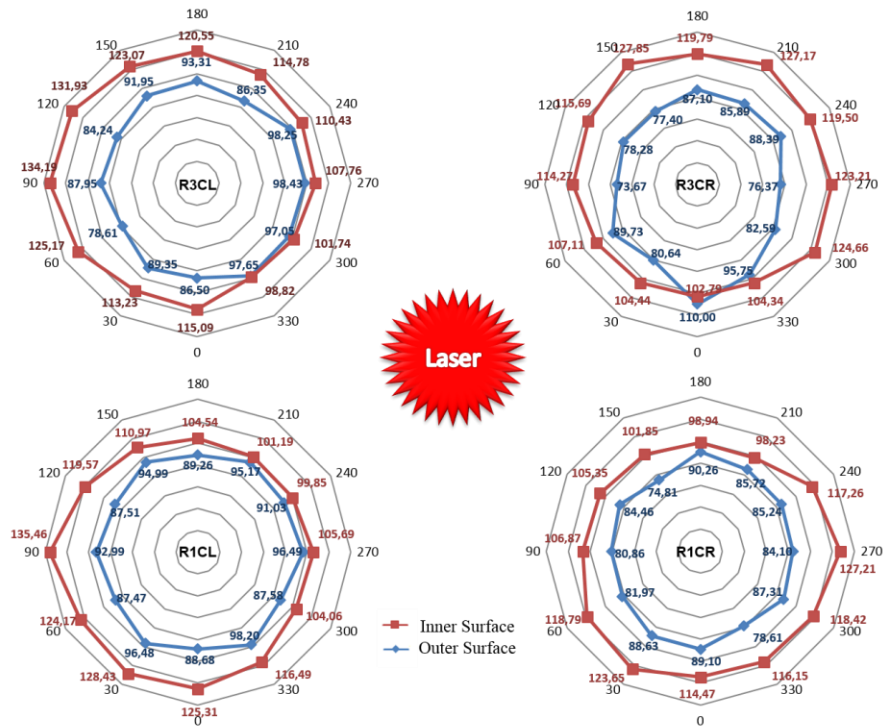


Figure 5: Prepared results of additional 45° specimen, which feature a thinner wall thickness of 0.5 mm in order to examine the impact of different thermal conductivity of heat. With a reduction of wall thickness the respective total area of the specimens cross section in z-direction becomes smaller. This was supposed to deteriorate the thermal conductivity during melting of powder, since most of the process heat is supposed to be conducted through the underlying solidified material.

The prepared measurements results from additionally thin walled specimen are depicted in Figure 5. Note that the thin walled specimen feature an overhanging angle of 45°. As can be seen from the figure, a similar tendency as observed for the previous 45° specimen can be observed for both, the inner and the outer surface (see Figure 3). Therefore, it can be assumed, that the size of the parts cross section, respectively the thermal heat conducting conditions, do not cause the observed effect of fluctuating surface roughness manifestations.

Figure 6 shows the results of additionally blast cleaned 45° specimen, taken from test series 1. Regarding the values of surface roughness a clear decrease can be noticed. Anyway, there is still a distinctive tendency of increased roughness visible for the outer surfaces. The slight tendency observed at the inner surfaces as previously noticed is no longer apparent. Moreover, the tendency at the outer surfaces seems to be stronger than before the blast cleaning. Now the roughness values are increased up to 40 µm.

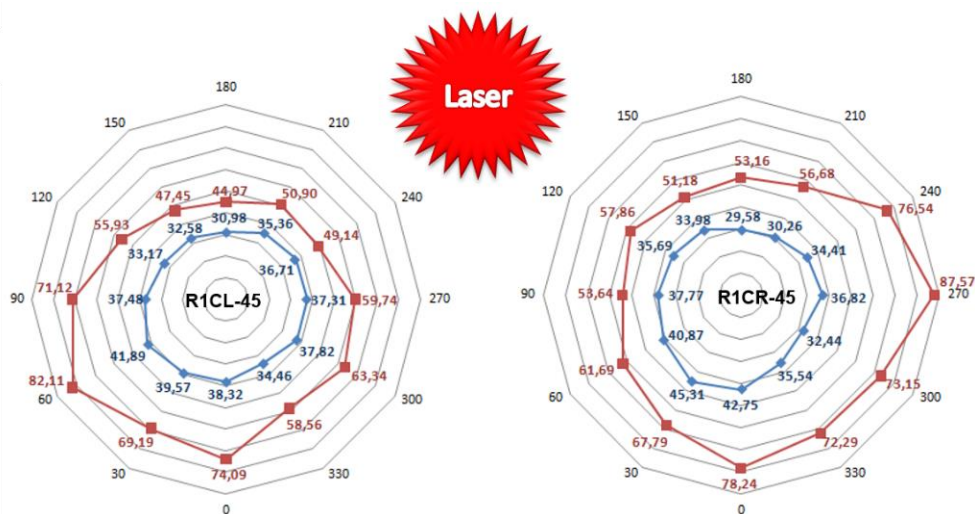


Figure 6: Additional specimens, which were taken from test series 1 and then blasted in order to investigate the influence of adherent powder particle to the observed tendencies of surface roughness manifestation. For Specimen designation see the inside of the polar plots.

Discussion

Results of our experimental study demonstrate that surface roughness of LBM components depends on position and orientation inside the process chamber. Additional specimens ruled out an influence of the different thermal conductivity situations, which are influenced by different sizes of the parts' cross section. Furthermore, the blast cleaned specimen showed, that the observed effect is not dominated by adhesion of powder particles. There are obviously physical effects during the melting and solidification, as mentioned in [13] and [15], which cause the observed tendencies. For understanding the causes of these effects it seems reasonable to take a look at the existing ancillary conditions. For all specimens process parameters and process conditions, like material, powder particle distribution, were identically. By using the selected specimen geometries, even the geometrical conditions of each specimen were known to be the same. The only thing that did vary during the build processes was the laser incidence angle. Due to the laser scanner system of LBM machines, the laser window is for logical reasons placed in the middle of the process chamber. Besides laser power, hatch distance, scanning velocity, layer thickness, etc. the laser focus diameter is also a relevant parameter for the defined energy input, and in consequence significant for the formation of the melt pool and resulting consolidation. As depicted in Figure 7a, the values of laser incidence angle significantly vary for different surfaces of the used specimen. From geometrical considerations it is obvious, that the laser beam is only circular in the middle of the process chamber. At every other position, especially in the corners and the sides, the shape of the laser beam might change into an elliptical form. In order to avoid this shape warping, most commercial LBM systems are equipped with F-Theta optics, which should ensure a uniform beam shape and scanning velocity at every position. One possible reason for the observed effect could therefore be found in small inaccuracies within the F-Theta optic.

Another possible reason could be different reflection conditions at different incidence angles. It could occur that the laser beam is directed onto the powder bed, like in Figure 7 shown at surface d. In this case, a larger proportion of laser beam intensity could be absorbed from the underlying powder material due to multiple reflections [4]. Thus, more energy input could occur at this surface, which could induct instabilities of the melt pool, balling, or melt extensions during solidification. In consequence a breakdown of the melt pool into the underlying powder bed could occur, which induces enhanced surface roughness after solidification. At the opposite surface - surface a in Figure 7a - these multiple reflections are probably impeded, due to the partially solidified underlying material. Figure 7b shows an enlarged representation of the incidence angle situation for surface c and d. Additionally the assumed heating situation is displayed qualitatively. For surface d the combination of overhanging and laser incidence angle is suspected to induce instabilities at the melt pool region. These instabilities could finally cause melt extensions, which are faced into the powder bed.

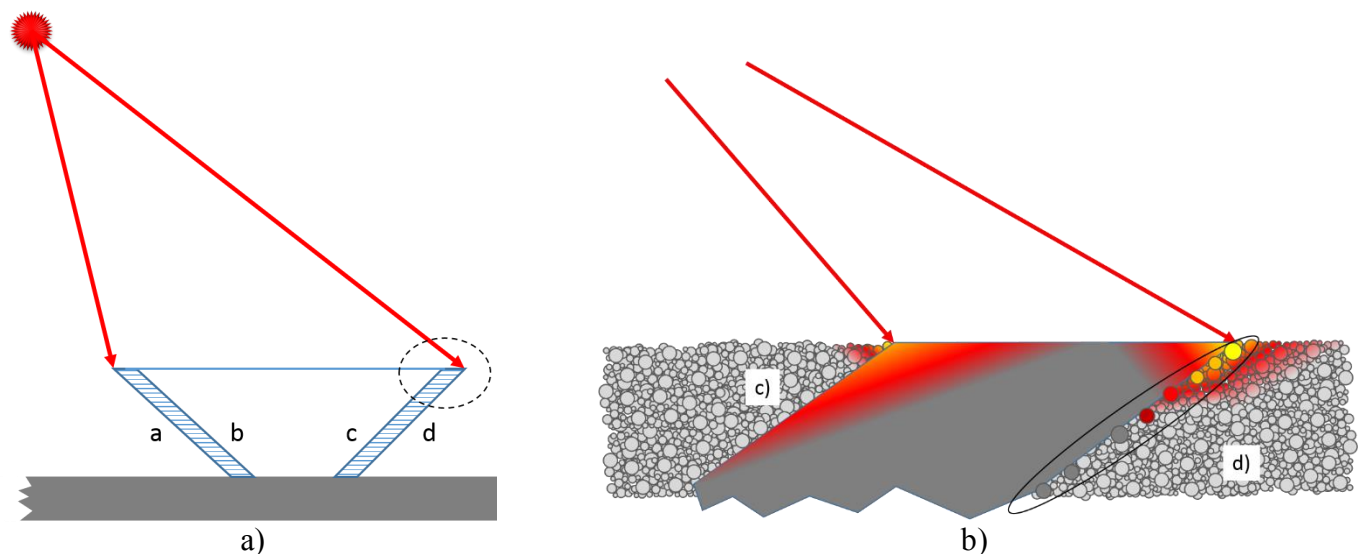


Figure 7: Schematic representation of the laser incidence angle situation for specimen R2CR-45. a): Sectional view of the test specimen. Due to the different surface orientations different laser incidence angles occur. b): Enlarged schematic representation for surfaces c and d. For surface d the laser beam points into the underlying powder material of the overhanging geometry. It is assumed that the observed deviations of surface roughness are related to wetting instabilities, which induce melt extensions into the powder material.

Figure 8 shows selected micrographs from a R2CR 45 specimen, which was built during a validation test series at MTU Aero Engines AG. According to the surface distinction in Figure 7 it is visible, that the surfaces a, b and c show no conspicuous features along the respective part surface, except some smaller adherent powder particle at surface a. At surface d two adherent extended structures are visible, which may be caused by balling or melt extension effects. Additionally these structures show some smaller adherent powder particles and feature a spherical structure. These structures seem to appear randomly, which may be connected with the rotated exposure strategy.

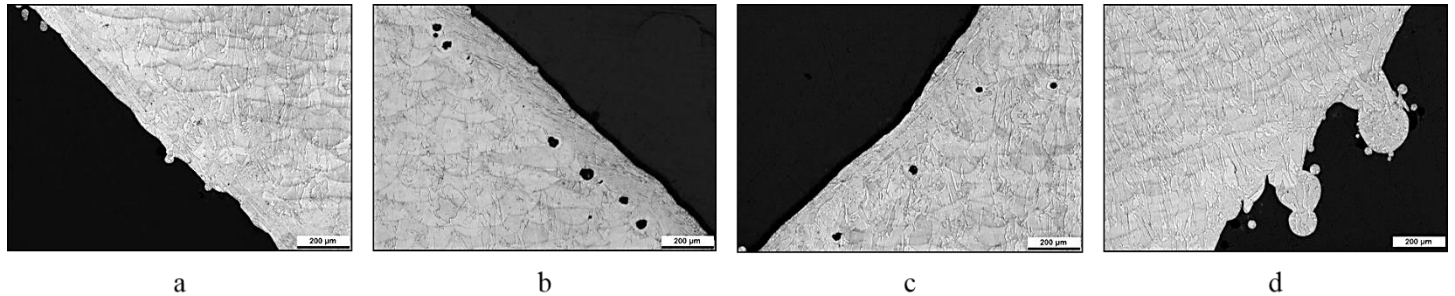


Figure 8: Selected micrographs from specimen R2CR-45, which was produced during validation of studies at MTU Aero Engines AG. According to the surface designation of figure 7 surface d shows some melt extensions, which seem to appear randomly. These melt extensions are assumed to be responsible for the observed deviations of surface roughness

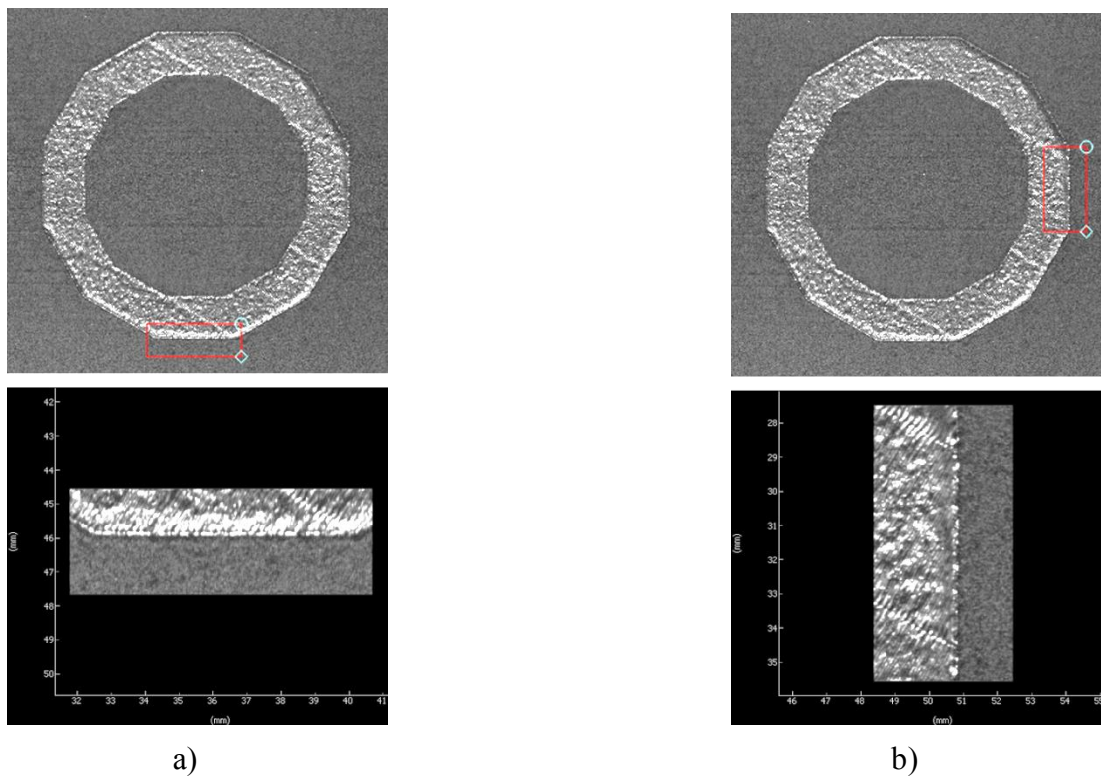


Figure 9: Selected images from process documentation during the experimental builds. Images were taken using a high resolution imaging system as presented in [10]. The upper images in a) and b) show the same picture, which was taken at a build height of 12.040 mm from test specimen R2CR-45-1. In both images different regions of interest were marked and additionally enlarged under the respective image of the test specimens' cross section. The enlarged view of the 270° surface in b) shows some interruptions at the contour region, which might be related to the before mentioned melt extensions. In a) the contour region seems to be much smoother and no interruptions are visible. Note the these observations were not apparent in every documented image, which might be related to inconsistent illumination and reflections of the molten regions.

As mentioned in section 3, a high resolution imaging system was used during the experimental build processes for process documentation purposes. As described in [10] and [11] the imaging system is able to resolve single melt traces in order to evaluate the process quality and stability. Figure 9 shows two selected images of specimen R1CR-45-2 which were taken during the LBM process after exposure in a build height of 12.040 mm.

The 0° surface in Figure 9a shows a quite uniform contour region. On the other hand Figure 9b shows a zoomed view of the 270° surface, which shows irregularities at the contour region, which may be a hint to balling or melt extensions effects. It is stated that these observations do not appear in every layer of the build process. For further layer images, some irregularities are also visible at the 0° surface. So it is not possible to conclude that there is a detectable connection between the visible irregularities and the observed roughness deviations. Nevertheless, automatic image analysis could be a suitable tool for detecting irregularities at the surface linked to roughness deviations, and should therefore be considered for future work.

5. Conclusions

The conducted investigations were able to demonstrate a position and orientation dependency of surface roughness for LBM specimen. It became apparent, that different surface orientations and overhanging angles result in different surface roughness values. A clear tendency was observed for the outer surfaces of 45° overhanging specimen, which showed increased roughness values for surfaces, which faced away from the center of the process chamber. The surfaces of the 70° overhanging specimen showed also slight differences at the inner surfaces. Due to the experimental design and the constant boundary conditions it can be stated that the observed deviations of surface roughness are not connected to process parameters or other process related errors. It was assumed that the geometrical situation of the laser incidence angle in combination with different surface orientations could be a cause for the deviations. Depending on the specimens' position and surface orientation, the laser beam is directed into the powder bed. Micrographs showed, that a formation of melt extensions occurs at the mentioned regions. This could be an indication for instabilities during the wetting interaction of the melt pool with the already solidified material. In consequence a breakdown of the melt pool at the affected regions occurs, which forms melt extensions and thus increases the resulting surface roughness. This is underpinned by the images from process documentation, which were taken by a high resolution imaging system.

The expedient usage of LBM into industrial everyday production requires precise information of the resulting mechanical properties and furthermore a high degree of reproducibility. The presented work has shown, that some process aspects need still improvement and are relevant for process preparation. In the present case the observed deviations have to be considered during batch production of multiple functional parts. Functional surfaces, with high requirements on surface quality, should therefore be placed and oriented in a way which prevents that the laser beam is directed into the powder bed. To obtain a more detailed understanding of the observed deviations further studies are necessary which illuminate the influence of different beam profiles and exposure strategies. Furthermore suitable process monitoring systems are crucial tools to understand the origin of the roughness deviations. In the present case high resolution imaging is suspected to be a suitable instrument for the evaluation of the affected regions at the parts' contours.

6. References

- [1] I. Gibson, D. W. Rosen und B. Strucker, Additive Manufacturing Technologies, New York: Springer, 2010.
- [2] Spierings, A. B.; Herres, N.; Levy, G., Influence of the Particle Size Distribution on Surface Quality and Mechanical Properties in Additive Manufactured Stainless Steel Parts, Austin, TX, USA: Proceedings of the Solid Freeform Fabrication Symposium, 2010.
- [3] J. T. Sehr, Möglichkeiten und Grenzen bei der generativen Herstellung metallischer Bauteile durch das Strahlschmelzverfahren, Dissertation, Universität Duisburg-Essen, 2010.
- [4] W. Meiners, Direktes Selektives Laser Sintern einkomponentiger metallischer Werkstoffe, Aachen: Shaker Verlag, 1999.
- [5] A. Spierings, K. Wegener und G. Levy, Designing Material Properties Locally with Additive Manufacturing Technology SLM, Austin, TX, USA: Proceedings of the Solid Freeform Fabrication Symposium 2012, 2012.
- [6] J. Bamberg, K.-H. Dusel und W. Satzger, „Overview of Additive Manufacturing Activities at MTU Aero Engines,“ in *AIP Conference Proceedings 1650*, 2015.

- [7] G. Zenzinger, J. Bamberg, A. Ladewig, T. Hess, B. Henkel und W. Satzger, „Process Monitoring of Additive Manufacturing by Using Optical Tomography,“ in *AIP Conference Proceedings 1650*, 2015.
- [8] N. N., „Opto Engineering,“ 2015. [Online]. Available: <http://www.opto-e.com/laser-resources-theory.php>. [Zugriff am 28 05 2015].
- [9] J. H. Schleifenbaum, J. Theis, W. Meiners, K. Wissenbach, A. Diatlov, J. Bültmann und H. Voswinckel, High Power Selective Laser Melting (HPSLM) - Upscaling the Productivity of Additive Metal Manufacturing towards Factor 10, Austin, TX, USA: Proceedings of the Solid Freeform Fabrication Symposium, 2010.
- [10] Kleszczynski, S.; zur Jacobsmühlen, J.; Sehr, J. T.; Witt, G., Error Detection in Laser Beam melting Systems by High Resolution Imaging, Austin, TX, USA: Proceedings of the Solid Freeform Fabrication Symposium, 2012.
- [11] S. Kleszczynski, J. zur Jacobsmühlen, J. T. Sehr, B. Reinartz und G. Witt, „Improving Process Stability of laser Beam melting Systems,“ in *Fraunhofer Direct Digital Manufacturing Conference (DDMC)*, Berlin, 2014.
- [12] G. Strano, L. Hao, R. Everson und K. Evans, „Surface Roughness Analysis, Modelling and Prediction in Selective Laser Melting,“ *Journal of Materials Processing Technology 213*, pp. 589 - 597, 2013.
- [13] J.-P. Kruth, G. Levy, F. Klocke und T. H. C. Childs, Consolidation phenomena in laser and powder bed based layered manufacturing, *Annals of the CIRP Vol. 56/2.* , 2007.
- [14] K. Mumtaz und N. Hopkinson, „Top Surface and Side Roughness of Inconel 625 Parts Processed Using Selective Laser Melting,“ *Rapid Prototyping Journal Vol. 15 Iss: 2*, pp. 96 - 103, 2009.
- [15] C. Körner, A. Bauereiß und E. Attar, „Fundamental Consolidation Mechanisms during Selective Beam Melting of Powders,“ *Modelling and Simulation in Material Science and Engineering 21 085011*, 2013.
- [16] Krauss, H.; Eschey, E.; Zäh, M. F., Thermography for Monitoring the Selective Laser Melting Process, Austin, TX, USA: Proceedings of the Solid Freeform Fabrication Symposium, 2012.
- [17] N. N., *DIN EN ISO 4287: Geometrical Product Specifications (GPS) – Surface texture: Profile method – Terms, definitions and surface texture parameters*, Berlin: Beuth Verlag, 2010.
- [18] N. N., *DIN EN ISO 4288: Geometrical Product Specifications (GPS) - Surface texture: Profile method - Rules and procedures for the assessment of surface texture*, Berlin: Beuth Verlag, 1998.